Luminescent liquid crystals: from supramolecular plant dyes to emissive flavylium salts

Robert Forschner, Julius Agamemnon Knoeller, Anna Zens, Wolfgang Frey, Yann Molard, Sabine Laschat

Luminescent Liquid Crystals: from Supramolecular Plant Dyes to Emissive Flavylium Salts

Robert Forschner,[a] Julius Agamemnon Knöller,[a] Anna Zens,[a] Wolfgang Frey,[a] Yann Molard,[b] and Sabine Laschat*,[a]

[a] *Institut für Organische Chemie, Universität Stuttgart, Pfaffenwaldring 55, D-70569 Stuttgart, Germany*

[b] *CNRS, ISCR, UMR 6226, ScanMAT – UMS 2001, University of Rennes, Rennes, France*

Dedicated to Prof. Dr. Klaus Roth for his contributions in chemical education and science for the public.

Abstract: Inspired by the supramolecular architecture of cornflower blue we developed luminescent flavylium salts with lipophilic alkoxy or thioether side chains which self-assemble into liquid crystalline phases. The current account highlights some fundamental aspects of our biological "role model" anthocyanine, the origin of the natural pigment cornflower blue, and our recent developments on novel liquid crystalline emissive dyes. Starting with the general synthesis of flavylium salts, other topics address variations of flavylium ILCs, including specific tuning of their mesomorphic and photophysical behaviour.

Keywords: flavylium salts, ionic liquid crystals, liquid crystals, Xray

Graphical Abstract:

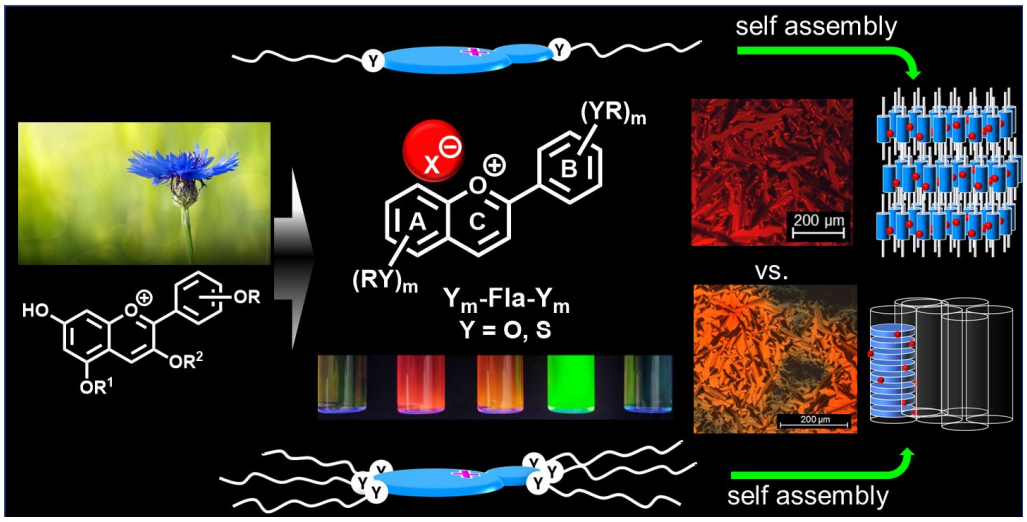

Introduction

The increasing demand for energy and resource efficient lighting for various household and technical applications has sparked a worldwide search for luminescent materials suitable for (organic) light emitting diodes. Luminescent materials which self-assemble into liquid crystalline phases have the additional benefit that the mesophase often facilitates homeotropic (face on) or planar (edge on) alignment on surfaces, shows self-healing of defects through thermal annealing, resulting in improved photophysical properties such as quantum yields and fluorescence/phosphorescence life times [1–3]. When looking for biological "role models" for novel luminescent liquid crystals we were attracted by anthocyanins, which are one of the most important families of plant dyes (Scheme 1). The colour of many flowers, fruits, berries and vegetables is caused by anthocyanins **1**, i.e. the glycosides of anthocyanidines **2** (the aglycons) [4–6]. The chromophoric flavylium core of anthocyanins **1** determines the absorption and emission colour, while the phenolic hydroxy groups serve as auxochromic groups shifting the absorption and emission bands and act as anchor points for glycosides, which enhance the solubility and stability of these plant dyes [7–9]. An overview of different prominent examples is given in Scheme 1. An amazing feature of this class of plant dyes is that the same anthocyanin displays different colours in different organisms. For example, cyanidin **3** appears red in roses but deep blue in cornflowers. The detailed understanding of the origin of these colours might not only be relevant for the use of anthocyanins as analytical markers in foodstuffs [10–12], as food colorants and photoprotectors [13] but also for bio-imaging and therapy of cancer cells [14] as well as novel materials for light emitting diodes or photovoltaic devices [15]. The structure elucidation of cornflower blue can be considered as a walk through a chemical maze. In this account we will briefly present some details of this chemical maze, which led us to conclude that the supramolecular architecture of cornflower blue might serve as guideline for the development of self-assembling liquid crystalline flavylium salts, which are sufficiently stable for further elaboration.

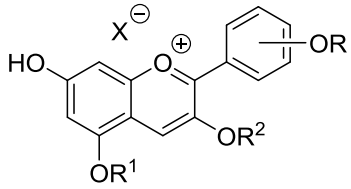

anthocyanin **1** R^1, R^2 = Glc
anthocyanidin **2** R^1, R^2 = H

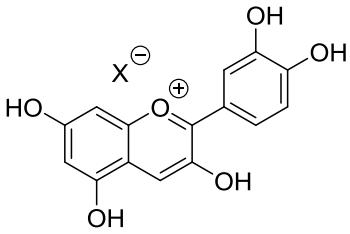

cyanidin **3**

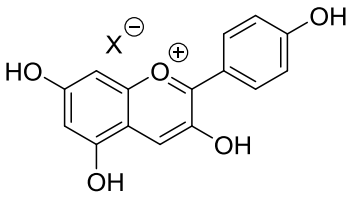

pelargonidin **4**

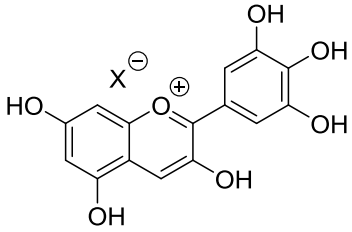

delphinidin **5**

Scheme 1. An overview of different anthocyanins. It should be noted, that in the literature the counterions of the naturally occurring anthocyanins were not specified.

Cornflower blue – a brief walk through the chemical maze of anthocyanins

Willstätter discovered already in 1913 the pH-dependent equilibrium between cyanin cation **6a** (pH = 1, red), neutral cyanine anhydrobase **6b** (pH = 4 – 6, purple) and the cyanin anion **6c** (pH = 7 – 9, deep blue) (Scheme 2) [16]. Somewhat later Shibata proposed that the cyanin anion forms a chelate complex **7** with Ca^{2+} or Mg^{2+} (Scheme 2) [17]. In 1939 Robinson and Robinson suggested that the cornflower blue originates from colloidal particles with metal ions [18]. More than 25 years later Bayer and coworkers isolated protocyanin, a high molecular weight compound after purification on Sephadex columns.

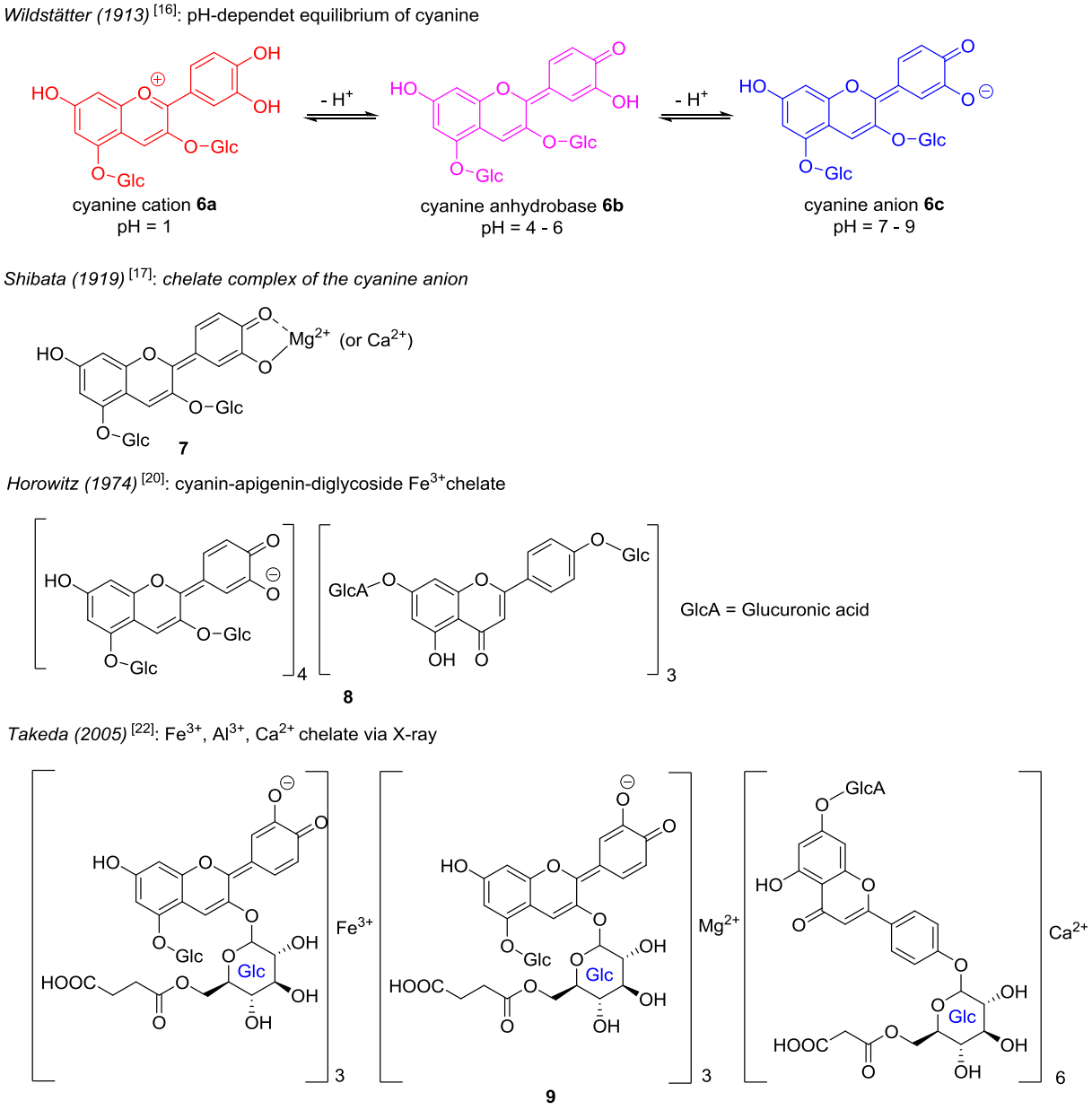

Scheme 2. Milestones in anthocyanine discovery.

Via ultrazentrifugation the diffusion constant of $12 \cdot 10^{-7}$ cm^2/s was determined [19]. Somewhat later Asen and Horowitz disclosed a cyanin-apigenin-diglycoside Fe^{3+} chelate **8** in order to rationalize the structure of cornflower blue (Scheme 2) [20]. Almost 20 years later Kondo, Goto and coworkers were able to obtain a high resolution mass spectrum of protocyanin, whose mass *m/z* 8511 g/mol was assigned to the species $C_{366}H_{384}O_{228}FeMg$ [21]. Based on this and prior evidence cornflower blue was proposed to exist as a supramolecular pigment. The race through the chemical maze culminated in 2005, when Shiono and

coworkers were able to solve the single crystal X-ray structure of cornflower's blue Fe^{3+}, Al^{3+}, Ca^{2+} chelate **9** (Scheme 2, Figure 1) [22].

As shown in Figure 1, the solid state structure revealed that cornflower blue is indeed a supramolecular pigment consisting of alternating Fe^{3+}, Al^{3+} and Ca^{2+} chelates **9** of cyanin malonate and cyanin succinate respectively (Figure 1a). Moreover, the helical stacking of the cyanin anions in the solid state were in good agreement with earlier NOE experiments in D_2O published by Kondo, Goto and coworkers (Figure 1b) [23].

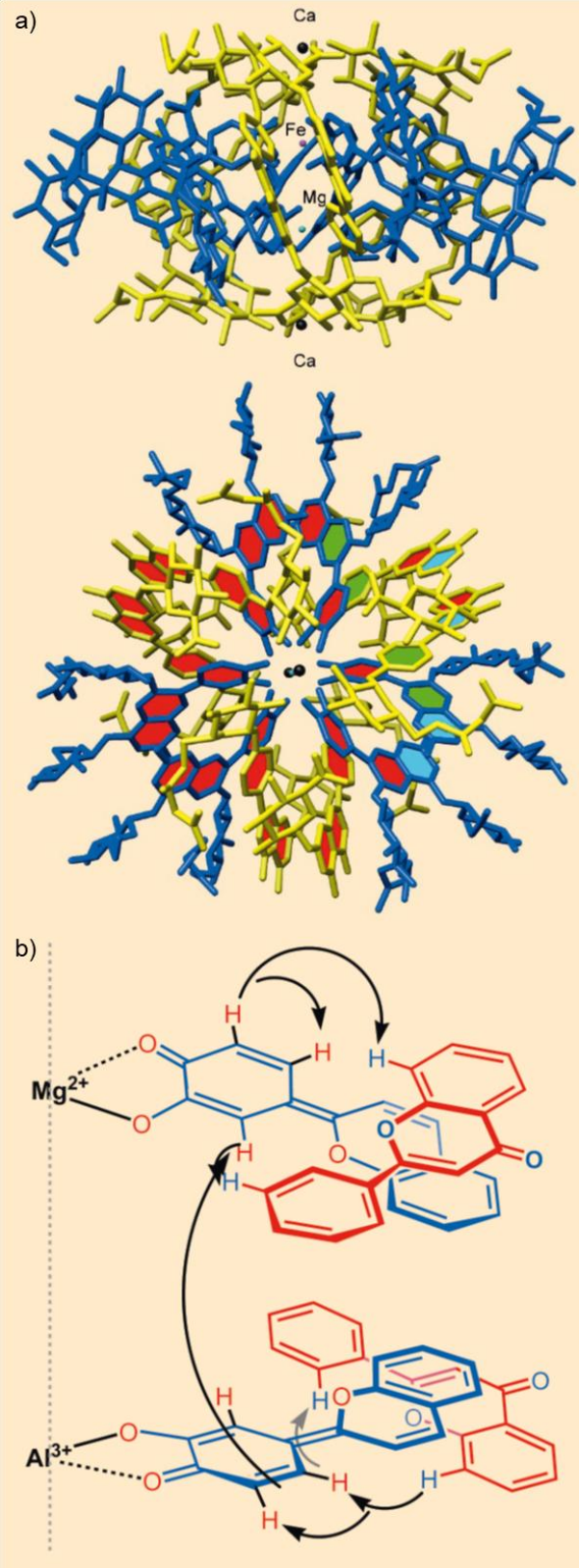

Figure 1. a) X-ray crystal structure of alternating Fe^{3+}, Al^{3+} and Ca^{2+} chelates **9** of cyanin malonate and cyanin.[22,24]; b) helical stacking of cyanin anions in the solid state confirmed by NOE experiments.[23] The Figure was taken and adapted from ref. [6] with permission from John Wiley and Sons.

As the water-soluble anthocyanins strongly favor the formation of columnar supramolecular aggregates via metal chelation and π-π interaction both in aqueous solution as well as in the bulk crystalline state we asked ourselfes whether flavylium salts carrying a charge in the center of the molecule and flexible hydrophobic side chains would lead to bulk columnar liquid crystalline self-assembly (Scheme 3). Such flavylium salts can be grouped into the steadily growing class of ionic liquid crystals (ILCs) [25–32].

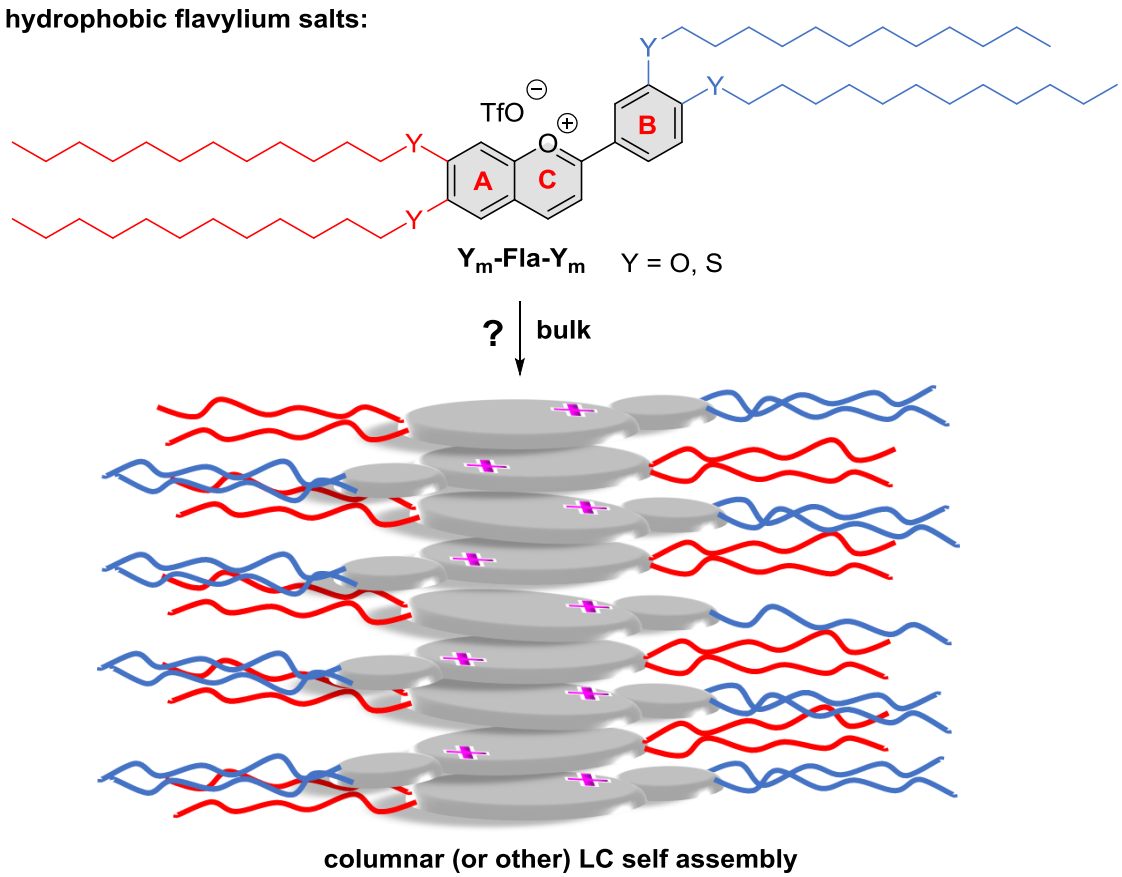

Scheme 3. Proposed bulk self-assembly of hydrophobic flavylium salts.

State of the art on pyrylium ILCs

The major difference between ILCs and classical non-charged thermotropic liquid crystals is the strong influence of the Coulomb interaction on the nanoseggregation and mesophase formation [25–32]. This electrostatic interaction together with van der Waals interaction, π-π interaction, hydrogen bonding and minimization of free volume leads preferably to lamellar

(SmA) as well as columnar (Col_h, Col_r) phases, while tilted phases such as SmC or nematic (N) phases are very rare among ILCs contrary to the classical non-charged liquid crystals [25–32].

It should be noted that not much work has been published on thermotropic flavylium or the parent pyrylium salts. Seminal investigations by Veber and coworkers showed that 2,6-diarylpyrylium salts **10** displayed a SmA phase [33] (Scheme 4). Later they extended their studies towards 2,6-diaryl and 2,4,6-triaryl pyrylium salts e.g. **11** with different substitution patterns, which led to the formation of Col_{ho} phases [34–36]. In addition, photophysical properties [37,38] and Langmuir-Blodgett films [39] were examined. Veber and coworkers also developed dimeric 2,4,6-triarylpyrylium salts **12** with monotropic Col_h phases [40]. More recently, Müllen disclosed condensed xanthylium derivative BNAX **13** forming Col phases [41]. With respect to flavylium salts only one report by Timmons on structurally related, neutral flavanones **14** with nematic and smectic mesophases existed in the literature [42].

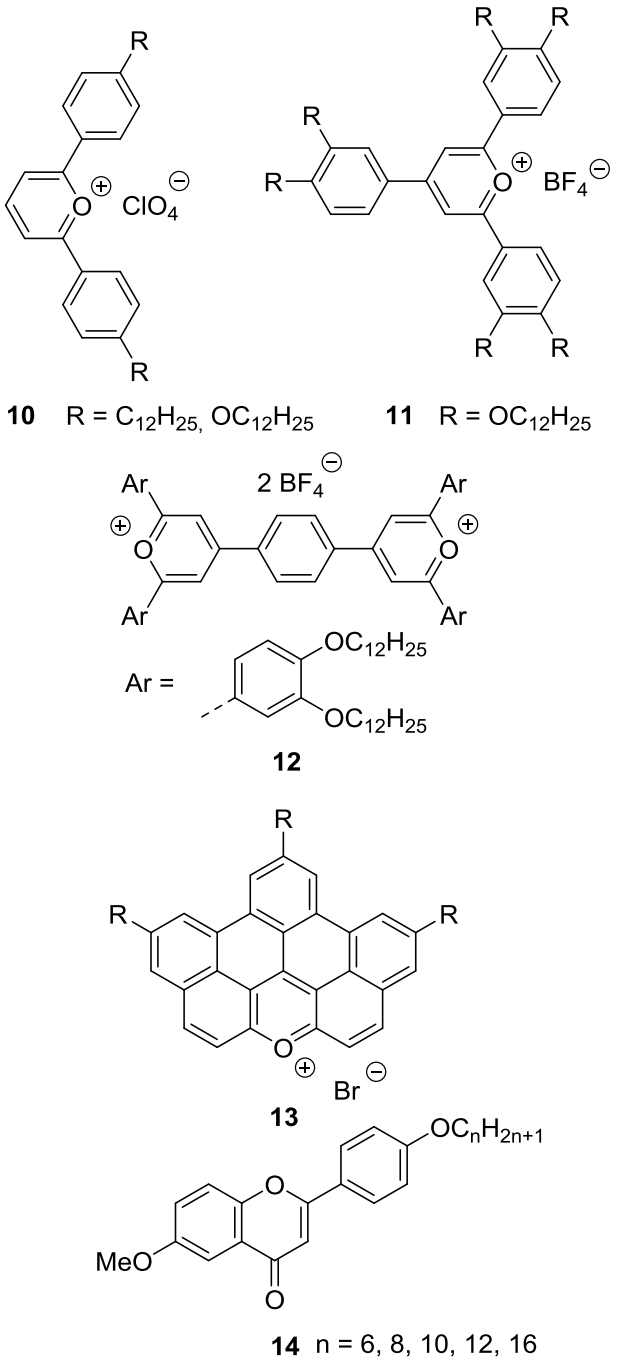

Scheme 4. Overview of thermotropic flavylium or pyrylium salts [43].

Upon comparison of flavylium salts with other ILCs another unique structural feature of flavylium salts is that the cationic charge is located more or less in the center of the molecule in contrast to the majority of ILCs where the cationic (or anionic) charge is located in the periphery and therefore is often designated as “head group”.[25–32] We expected that this central positive charge together with the counteranion and the O (or S) atoms connecting the

side chain with the aromatic core might be relevant for both mesophase formation and photophysical properties.

In the following brief account we will showcase for selected amphiphilic flavylium salts how their solid state structure is correlated with their liquid crystalline structure. Furthermore, we will outline the influence of their supramolecular aggregation both in solution, the bulk state and liquid crystalline state on their luminescence properties.

Our own contributions to flavylium ILCs

As outlined in Scheme 5 synthetic access towards flavylium salts is straightforward using alkoxybenzaldehydes as starting material. Alkoxybenzaldehydes **17** which are available from a series of hydroxybenzaldehydes **15** by Williamson etherification can be converted to the phenols **19** by Dakin oxidation.[44] On the other hand, Grignard addition of ethinylmagnesium bromide to alkoxybenzaldehyde **17** yields the propargylic alcohol **18**, which is oxidized to the corresponding ketone **20**. Phenols **19** and propargylic ketones **20** are then condensed under acid mediation to yield the desired flavylium salts $\mathbf{Y_m}$**-Fla-**$\mathbf{Y_m}$ (Y = O, S; m = 1, 2, 3). Starting from the alkoxy-substituted aldehyde **17** a library of 23 different flavylium salts (R = $C_{12}H_{25}$) is available [43], enabling different degrees of space filling. The sequence towards the thioether-substituted flavylium salts $\mathbf{S_m}$**-Fla-**$\mathbf{S_m}$ is similar except for the initial introduction of the thioether side chain, which was achieved by nucleophilic displacement of fluoride [45] following protocols by Jankowiak [46] and Prasad [47].

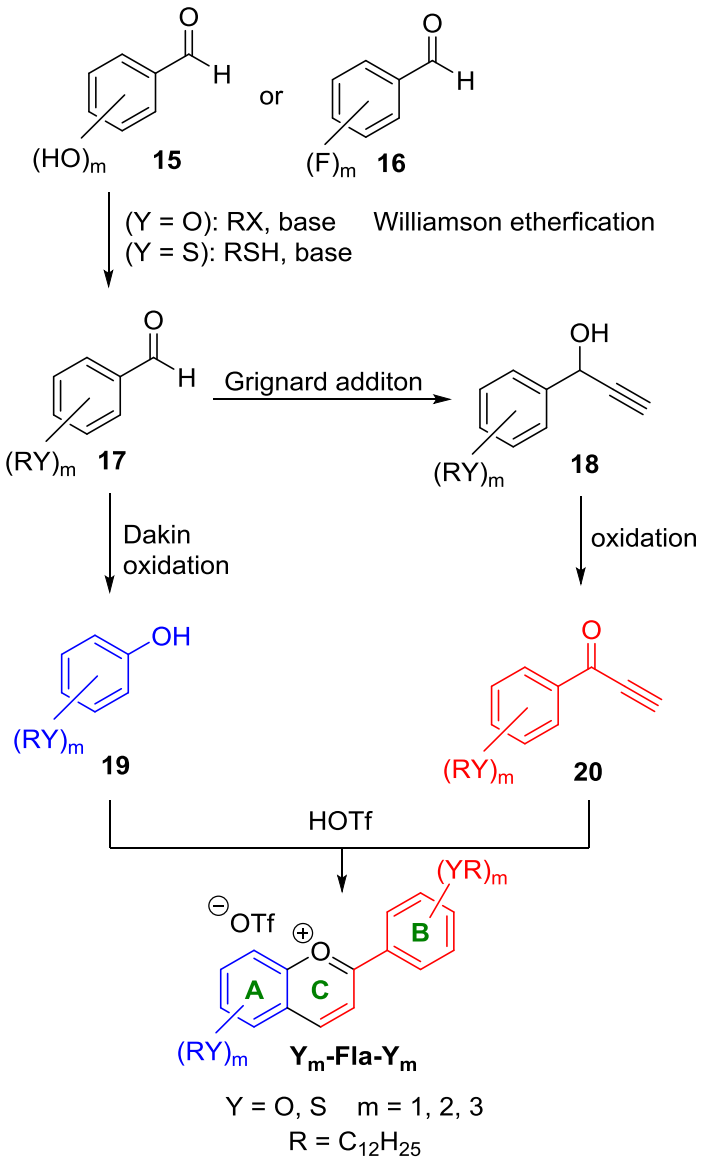

Scheme 5. General synthesis of alkoxy- and thioether-substituted flavylium salts.[43,45]

Comparison of the single crystal X-ray structures of vanillin-derived flavylium salts **O_1-V-Fla-O_1** (Figure 2a) and **O_1-V-Fla-S_1** (Figure 3a) carrying only one side chain on each A and B ring respectively, provided insight into the solid state packing (Figures 2, 3).[43,45] For **O_1-V-Fla-O_1** an antiparallel packing of two neighboring chromenylium units (AC-ring) was observed with a π-π stacking distance of 3.56 Å between the pyrylium cores and a somewhat longer distance of 3.66 Å between the centroids (Figure 2b). The corresponding distances for **O_1-V-Fla-S_1** are 3.50 Å and 3.78 Å respectively (Figure 3b). Thus, the increased steric demand of the thioether chain in the latter case pushes the centroids farther away from each

other. In both O- and S-compound the flavylium cation is nearly planar with a slightly larger torsion angle for the S-compound (6.9°) as compared to the O-compound (5.0°). Both flavylium salts form a lamellar arrangement (along the *c*-axis) with a polar sublayer alternating with a non-polar layer of the alkyl chains, which are strongly interdigitated. **O_1-V-Fla-O_1** and **O_1-V-Fla-S_1** are stabilized by H-bonds. From Figures 2,3 it is obvious that the most significant difference between the O- and S-compound is the smaller bond angle of the thioether 4'-S-CH_2 (106.2°) as compared to the bond angle of the alkoxy derivative 4'-O-CH_2 (118.5°), resulting in a stronger bending of the molecular structure of **O_1-V-Fla-S_1** as compared to **O_1-V-Fla-O_1**.

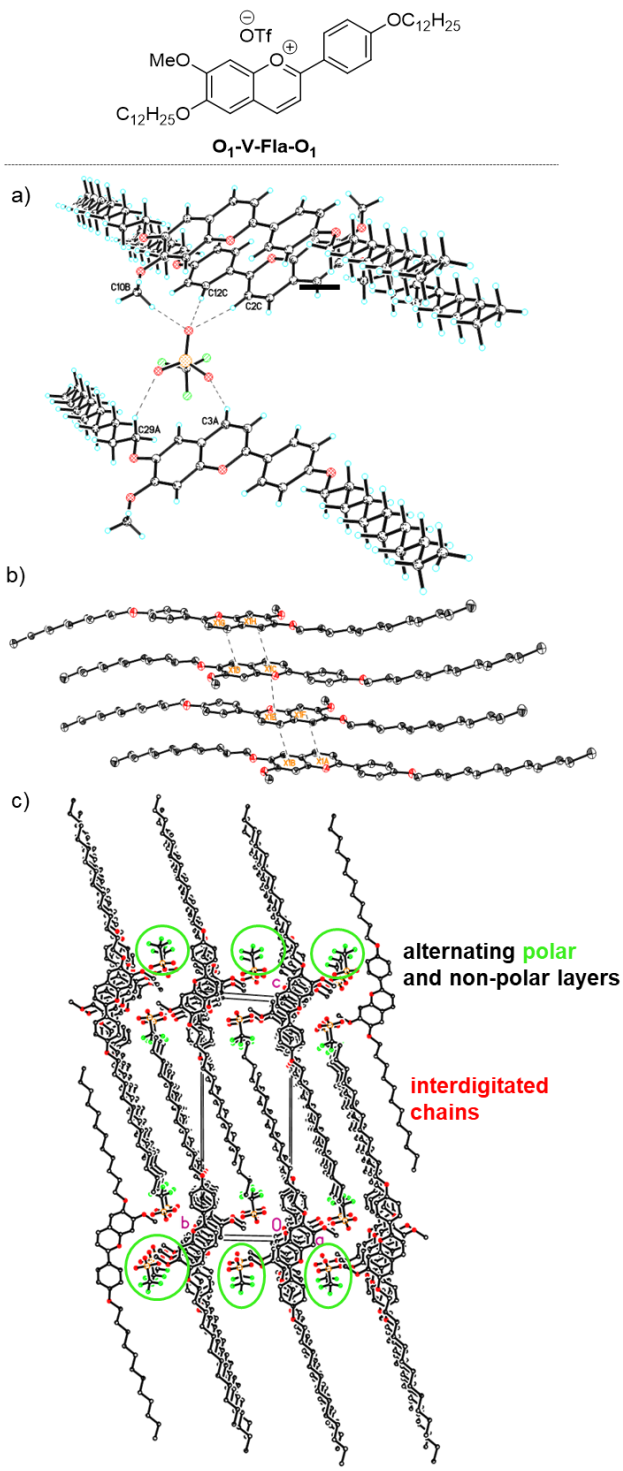

Figure 2. Single-crystal X-ray structure of **O_1-V-Fla-O_1** in the solid state (H = lightblue, C = white, O = red, S = yellow, F = green, in b) and c) hydrogens are omitted for clarity); a) intermolecular hydrogen bonds with triflate by dashed lines; b) π–π–interaction of the flavylium cation; c) *bc* view along the *a* axis showing the interdigitated layer structure. The figure was taken from ref. [43] and modified. This is an open access article distributed under the terms of the Creative Commons CC BY license, which permits unrestricted use, distribution, and reproduction in any medium, provided the original work is properly cited.

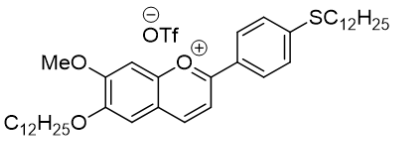

O_1-V-Fla-S_1

a)

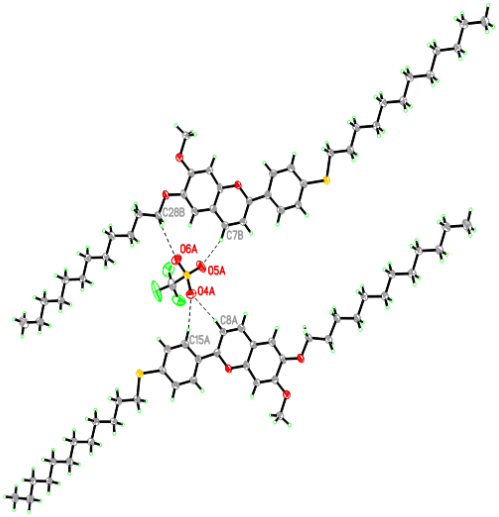

b)

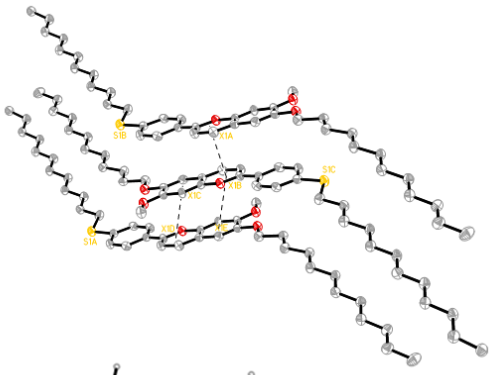

c)

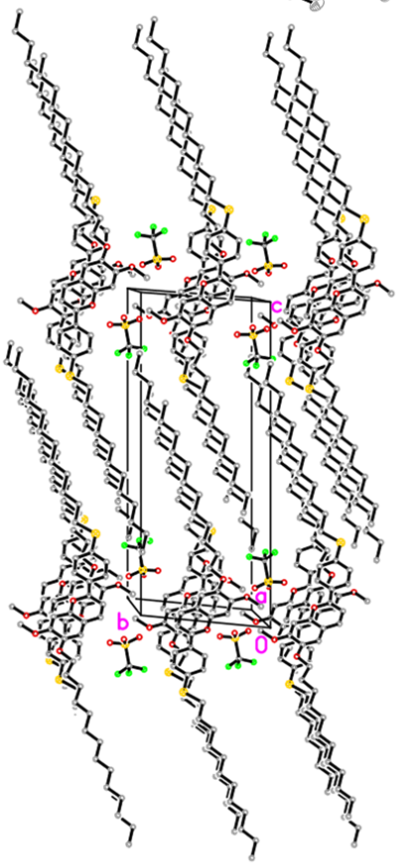

Figure 3. Single-crystal X-ray structure of **O_1-V-Fla-S_1** in the solid state (H = lightblue, C = grey, O = red, S = yellow, F = green, in b) and c) hydrogens are omitted for clarity): a) intermolecular hydrogen bonds with triflate by dashed lines and b) π–π–interaction of the flavylium cation. c) *bc* view along the *a* axis showing the interdigitated layer structure. The figure was taken from ref. [45] and modified. This is an open access article distributed under the terms of the Creative Commons CC BY license, which permits unrestricted use, distribution, and reproduction in any medium, provided the original work is properly cited.

With these informations on the solid state structure in hand we were curious whether similar packing would be observed for the rod-shaped members of the flavylium salt library. Indeed, as it turned out from DSC and POM investigations (Figure 4) calamitic flavylium salts with one or two side chains at the A ring and only one side chain at the B ring displayed SmA or lamellar columnar (Lam_{Col}) phases. [43,45] If more than one chain is attached to the B-ring, mesophase formation is either completely suppressed or shifted in favour of columnar phases.

Moreover, two thioethers at the A ring also prefer a columnar self-assembly. For derivatives **S_2-Fla-S_2**, **S_3-Fla-S_2** Col_{ho} phases were much broader and more stable as compared to the O-analogues. Thus, the mesophase type and temperature range can be tailored independently introducing thioethers to the A and B ring of the flavylium salts, respectively.

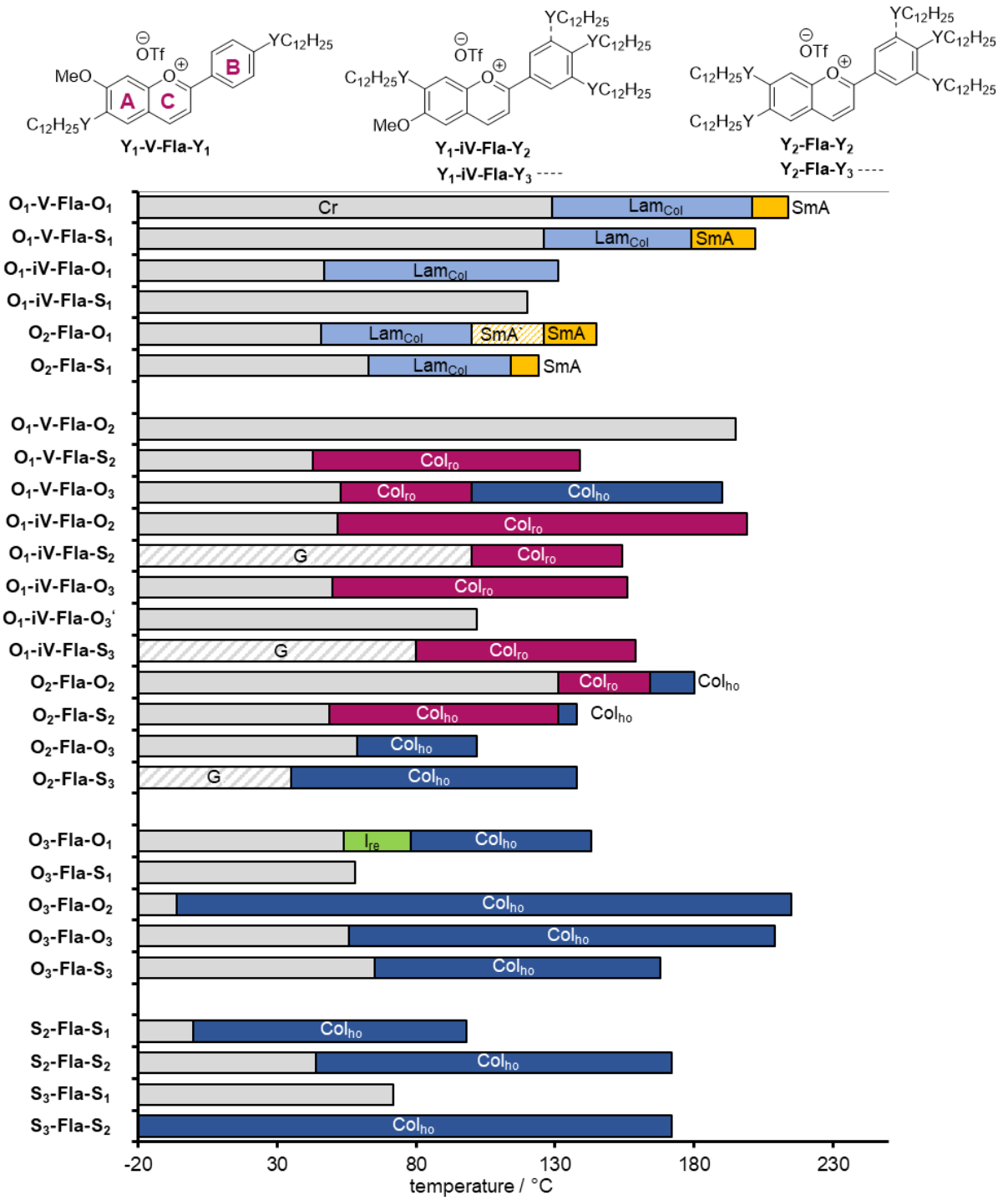

Figure 4. Mesophases of thioether flavylium salts **O_m-Fla-S_m** in comparison to their ether counterparts **O_m-Fla-O_m**;. Cr (crystalline; grey), G (glass), SmA (smectic A), SmA' (smectic A build up by dimers), Lam_{Col} (lamello columnar), Col_{ro} (columnar rectangular ordered), Col_{ho} (columnar hexagonal ordered). The figure was taken from ref. [43,45] and adapted accordingly.

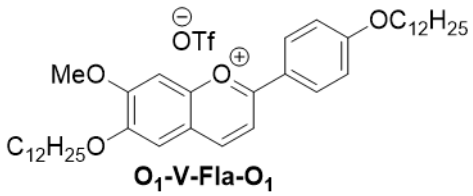
OTf
MeO
O
OC12H25
C12H25O

O_1-V-Fla-O_1

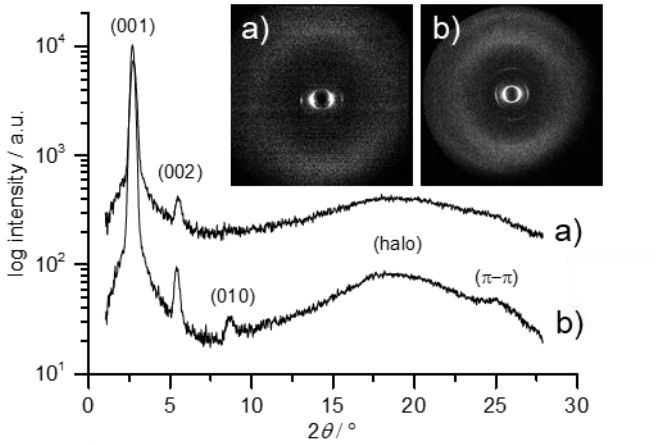
(001)
a)
b)
(002)
(halo)
(π–π)
(010)
a)
b)
log intensity / a.u.
2θ / °

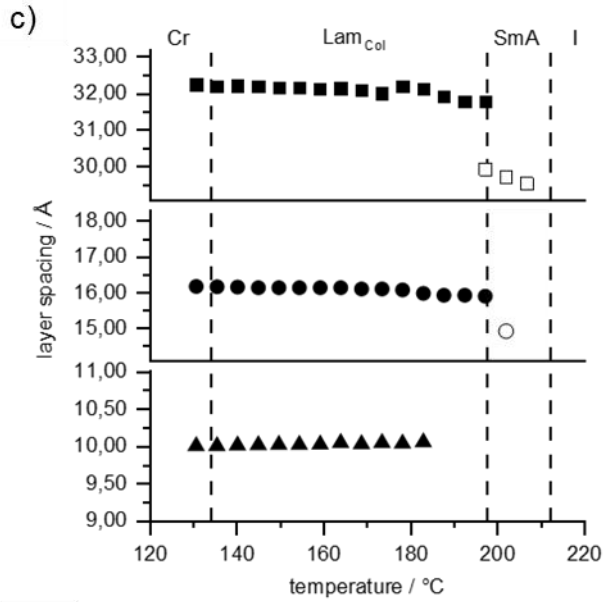
c)
Cr
Lam Col
SmA
I
layer spacing / Å
temperature / °C

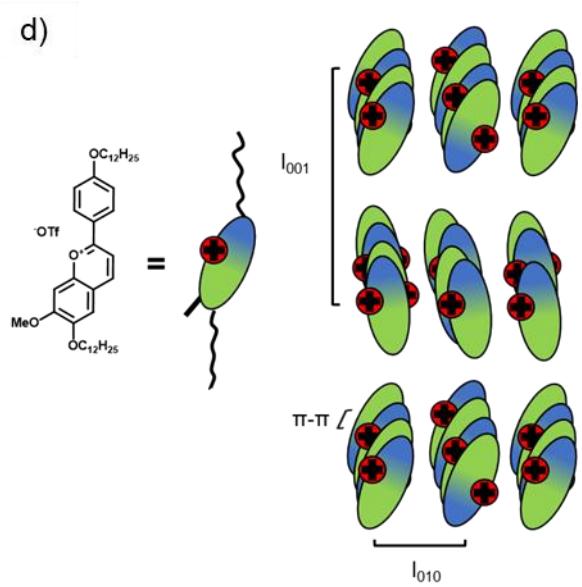
d)
OTf
MeO
I001
π-π
I010

Figure 5. Diffractogram and the diffraction pattern of the oriented sample of **O_1-V-Fla-O_1** in the SmA (top, a) and Lam_{Col} (bottom, b) mesophase after cooling from the isotropic state at 210 °C and 170 °C; c) Temperature dependent layer spacing of the (001) reflex (■), the (002) reflex (●)and the (010) reflex(▲) in the SmA (hollow symbols) and the Lam_{Col} phase(filled symbols) of **O_1-V-Fla-O_1**.The measurement was performed during the second heating (rate:2 K min^{-1}); d) Proposed packing of the molecules in the Lam_{Col} mesophase. The figure was taken from ref. [43] and modified.

As can be seen from the XRD data shown in Figure 5a,b for **O_1-V-Fla-O_1** the Lam_{Col} phase can be differentiated from the SmA phase via measurement of the temperature-dependent layer spacing, which remained relatively constant in the former case, but decreased more steadily in the latter case (Figure 5c). Presumably, the Coulomb interaction between the flavylium cation and triflate anion and the nanoseggregation of non-polar parts favoring SmA phase are partially overcompensated by the π-π interaction between the pyrylium (C-ring) and the AC-rings of neighboring molecules stabilizing the Lam_{Col} phase at the expense of the SmA phase (Figure 5d).

When comparing the XRD data of the calamitic flavylium salts carrying alkoxy chains in the B-ring with the corresponding ILCs with thioether chains, it is obvious that for both SmA and Lam_{Col} phase the layer distances are smaller for the S-compound, whereas the halo and π-π distances are larger. This might be rationalized as follows: the increased size of the S atom pushes the B-ring farther away from it's neighbor within the layer of the SmA or Lam_{Col} phase, thereby increasing the π-π distance, while simultaneously the alkyl chains are less densely packed. In order to compensate the free volume in the hydrophobic region the alkyl chains deviate from the all-*trans* conformation by extending their thermal fluctuations and thus the overall layer distance d_S decreases (Figure 6).

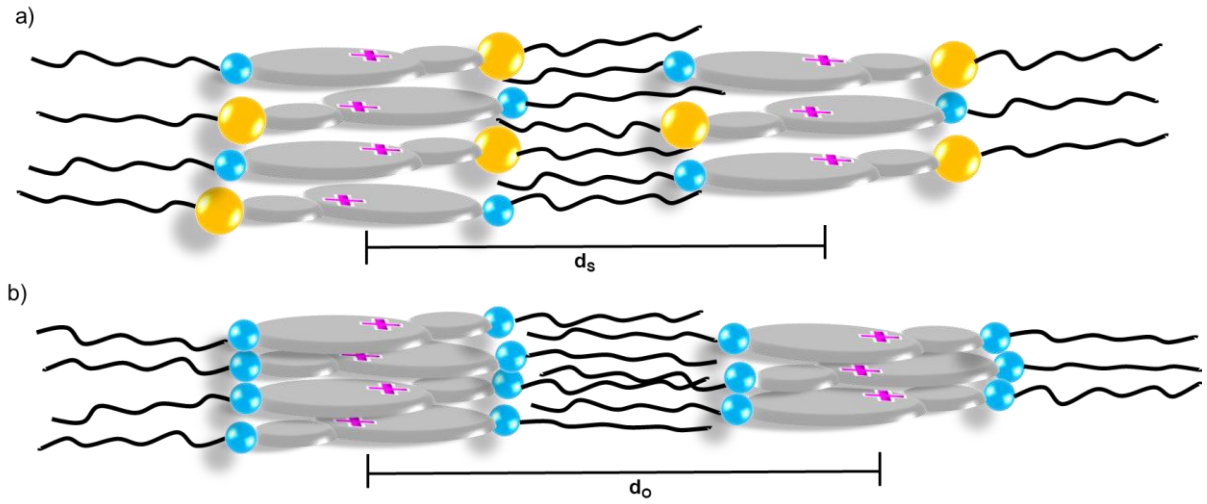

Figure 6. Proposed stacking interaction of flavylium cation a) **O_1-V-Fla-S_1** with thioether side chain in the B-ring in comparison to b) **O_1-V-Fla-O_1** with the corresponding alkoxy side chain.; The sulfur atoms are highlighted in yellow, the oxygen atoms in blue.

When the total number of side chains at the flavylium salts exceed 3, columnar mesophases are strongly favoured. In other words, deviation from the calamitic structure results in exclusive formation of columnar mesophases except for **O_1-iV-Fla-O_3'**, **O_3-Fla-S_3** and **S_3-V-Fla-S_1**, which are non-mesomorphic (Figure 4). In agreement with previous reports by Bruce on phasmidic liquid crystals and tetracatenar phenanthroline liquid crystals [48–50] flavylium ILCs with 3 and more side chains showed columnar rectangular (Col_{ro}) phases because minimization of free volume cannot be any longer achieved in a lamellar packing. While O-derivatives tolerated up to 5 side chains and still displayed Col_{ro} phases, for the bulkier S-derivatives the columnar hexagonal (Col_{ho}) phase becomes prevalent with 5 side chains. Flavylium salts with 6 side chains all formed Col_{ho} phases. Examples of borderline cases, where both Col_{ro} and Col_{ho} geometries can be accommodated are **O_1-V-Fla-O_3**, **O_2-Fla-O_2**,

O_2-Fla-S_2. For the latter case the two different geometries are illustrated in Figure 7.

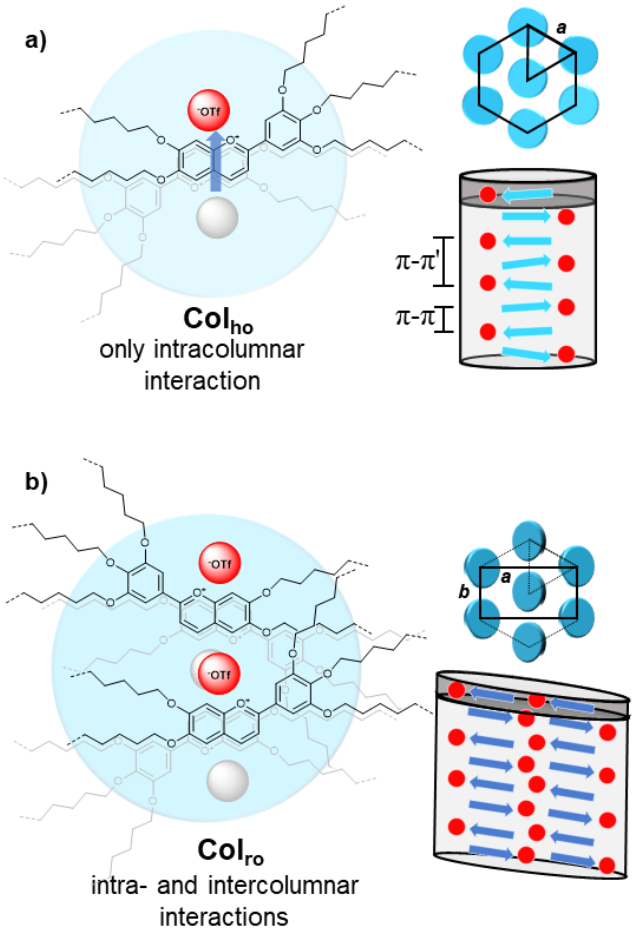

Figure 7. Proposed packing model of the flavylium salts in the a) Col_{ho} and the b) Col_{ro} mesophase viewed from the top (left) and in an side view (right). The flavylium cations are displayed as blue arrows (pointing towards the oxonium cation) and the triflate anions as red dots. The figure was taken from ref. [43] and modified. This is an open access article distributed under the terms of the Creative Commons CC BY license, which permits unrestricted use, distribution, and reproduction in any medium, provided the original work is properly cited.

In the Col_{ro} phase optimal space filling is achieved by accommodating two antiparallel oriented flavylium units per disk which are stacked along the column in an antiparallel fashion. The flavylium ions are separated by the corresponding counterions. In contrast, in the Col_{ho} phase each disk consists only one molecule stacked antiparallel along the column with the counterion being present in close proximity. Upon comparison of alkoxy-substituted flavylium ILCs with thioether-substituted ILCs the S-derivatives accommodate the larger

thioether chain in the unit cell of the Col_{ro} phase by stretching the *a*-axis, simultaneously shortening the *b*-axis and increased interdigitation of the alkyl chains. In contrast, for the Col_{ho} geometry the replacement of O vs. S resulted in tighter packing of the disks within the hexagonal lattice, thus the lattice parameter *a* is reduced, while the disks become "thicker" as the π-π distance increases (Table 2). It should be noted, that the strong tendency of flavylium salts to form columnar aggregates when carrying a sufficient number of side chains, was also observed in solution. Concentration-dependent chemical shifts in the NMR spectra of **O_1-iV-Fla-S_3** and diffusion coefficients obtained via DOSY spectra revealed oligomeric aggregates with different sizes in solution [45].

Table 2. XRD data of flavylium ILCs with more than 3 side chains

	mesophase	a [Å]	b [Å]	halo [Å]	anion [Å]	π–π [Å]
O_1-iV-Fla-O_2	Col_{ro}	50.0	35.9	4.71	3.52	3.44
O_1-V-Fla-S_2	Col_{ro}	50.3	34.3	4.62	3.49	3.43
O_1-iV-Fla-S_2	Col_{ro}	54.4	33.9	4.58	3.49	3.42
O_1-iV-Fla-O_3	Col_{ro}	51.0	36.3	4.63	4.06	3.39
O_1-iV-Fla-S_3	Col_{ro}	53.3	33.4	4.57	4.20	3.49

Flavylium ILCs with alkoxy side chains show characteristic absorption and emission properties in solution. As exemplified for vanillin-derived flavylium salts **O_1-V-Fla-O_m** (m = 0 – 3) in Figure 8 and Table 3, the absorption maxima are red-shifted from the parent system **O_1-V-Fla-O_0** with unsubstituted phenyl B-ring (λ_{max} = 444 nm) upon increase of the number of side chains at the B-ring (**O_1-V-Fla-O_3**, λ_{max} = 496 nm), whereas the substitution pattern on the A-ring had only minor influence.

Table 3. Photophysical data of alkoxy-substituted flavylium salts **O_1-V-Fla-O_m** in $CHCl_3$.

	λ_{max} [nm]	λ_{em} [nm]	Φ_F
O_1-V-Fla-O_0	444	505	0.04
O_1-V-Fla-O_1	484	521	0.97
O_1-V-Fla-O_2	501	570	0.05
O_1-V-Fla-O_3	496	593	< 0.01
O_1-V-Fla-O_3'	490	525	< 0.01

The corresponding fluorescence maxima were also red-shifted from λ_{em} = 505 nm for **O_1-V-Fla-O_0** to 593 nm for **O_1-V-Fla-O_3**. However, the most puzzling observation was, that only the O-derivative with one *p*-alkoxy chain at the B-ring possessed a high photoluminescence quantum yield (ϕ_F = 0.97), while all other members of the series displayed much lower ϕ_F values ($\phi_F \leq 0.05$). Similar observations were made for the series of S-derivatives. The slightly lower quantum yields of **O_1-V-Fla-S_1** (ϕ_F = 0.84) and **O_2-Fla-S_1** (ϕ_F = 0.86) as compared to the O-counterparts can be rationalized by the heavy atom effect, which led to complete quenching of the luminescence when thioethers are also present in the A ring.

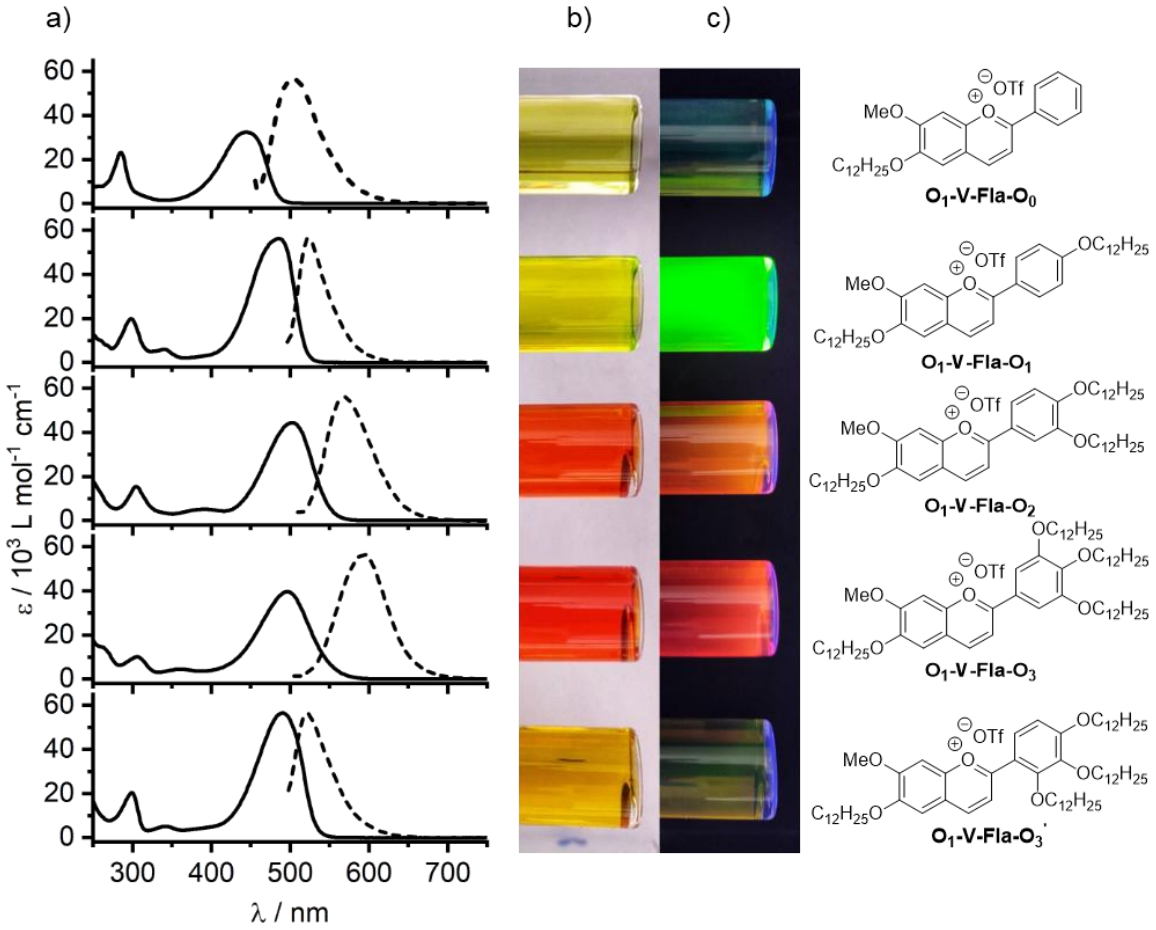

Figure 8. Absorption spectra (bold line, represented by its extinction co-efficient determined by linear regression of a concentration series ranging from $0.2x10^{-5}$ to $7x10^{-5}$ M) and normalized emission spectra (dashed line) of vanillin-derived flavylium salts in $CHCl_3$. Solutions of the corresponding flavylium salt under b) daylight and c) UV-radiation (366 nm). The figure was taken from ref. [43] and modified. This is an open access article distributed under the terms of the Creative Commons CC BY license, which permits unrestricted use, distribution, and reproduction in any medium, provided the original work is properly cited.

The unexpected high fluorescence intensity for derivatives carrying only one *p*-alkoxy (or *p*-thioether) chain at the B-ring and the pronounced decrease of ϕ_F values for all other members was rationalized based on previous TD-DFT calculations from Woodford on unsubstituted flavylium salts [51] and our complementary DFT calculations [43], which revealed that mesomeric Lewis structures **M1**, **M2** are favoured over **M0** in case of the unsubstituted B-ring allowing free rotation of the phenyl (B-ring) (Figure 9). However, the

+M effect of a *p*-alkoxy substituent at the B-ring stabilizes **M3**, resulting in partial C=C bond character of the bond between C and B-ring. This rigidification of the chromophor leads to enhanced quantum efficiency. On the other hand, any additional OR (or SR) group at the B-ring destabilizes this rigid structure **M3** (via –I effect) resulting in fluorescence quenching due to the increased rotational flexibility.

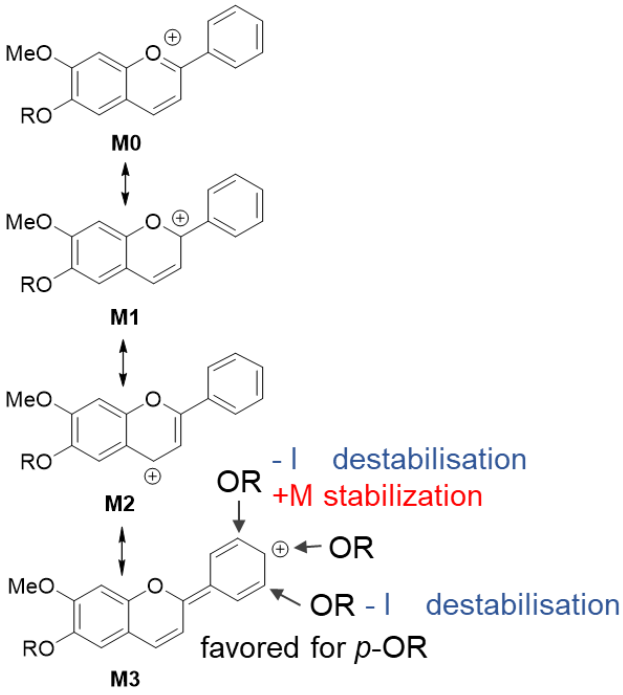

Figure 9. Possible mesomeric resonance structures.

As the molecular structure, i.e. the substitution pattern and type of connecting atoms (O vs S) affected the absorption and fluorescence properties in solution, we surmised that the supramolecular organization in the bulk state should also have an influence on the emission properties. The three flavylium salts **O_1-V-Fla-O_1**, **O_1-iV-Fla-O_1**, **O_2-Fla-O_1** with the highest emission intensity in solution were examined regarding their solid state emission (Figure 10a). All derivatives displayed a broad red-shifted emission at λ_{em} = 645 nm. However, when measuring the temperature-dependent emission intensity the three flavylium salts behaved differently (Figure 10b).

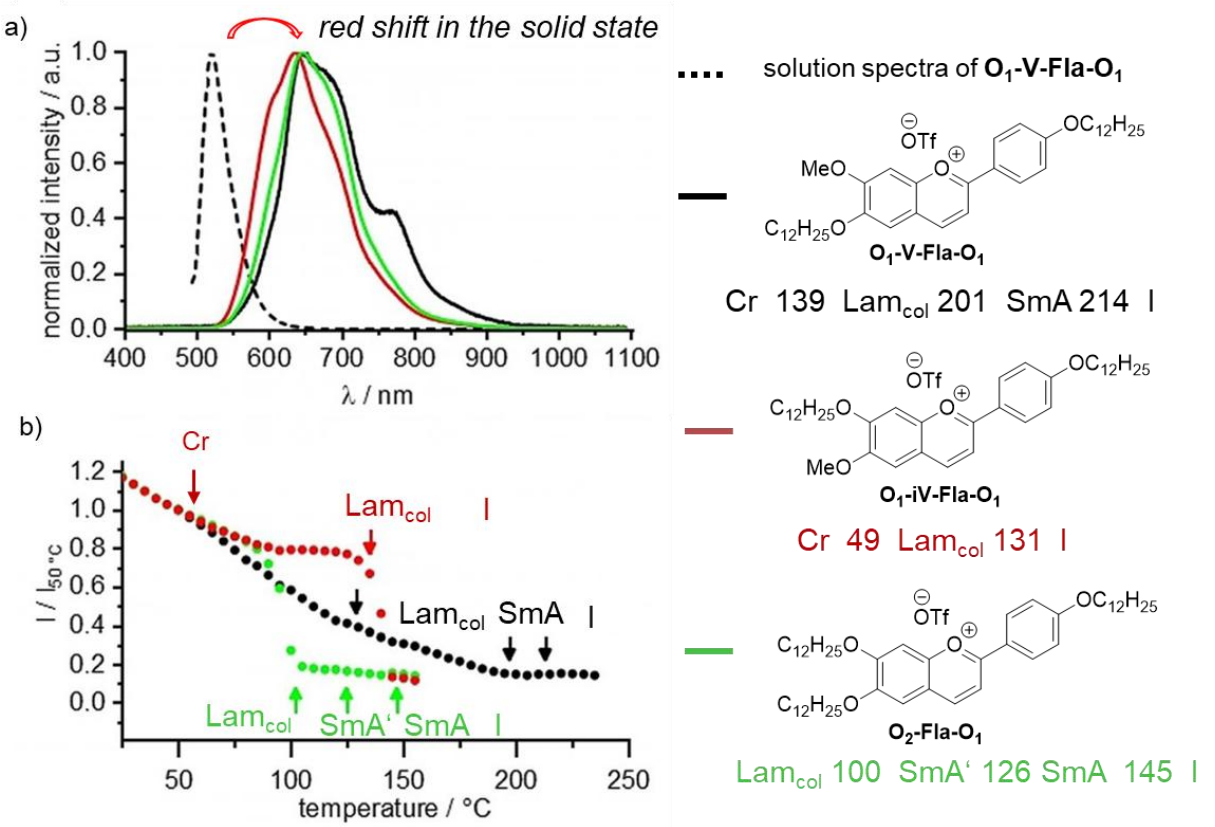

Figure 10. a) Emission spectra of **O_1-V-Fla-O_1** (black), **O_1-iV-Fla-O_1** (red) and **O_2-Fla-O_1** (green) in the solid state at 50 °C upon excitation with UV light (350 – 380 nm), solution spectrum of **O_1-V-Fla-O_1** is given in dashed lines for comparison and b) temperature-dependent emission intensity at 665 nm measured during cooling the sample from the isotropic liquid (cooling rate of 10 $Kmin^{-1}$). For the orientation transition temperatures of the DSC are given as arrows.The figure was taken from ref. [43] and modified. This is an open access article distributed under the terms of the Creative Commons CC BY license, which permits unrestricted use, distribution, and reproduction in any medium, provided the original work is properly cited.

For **O_1-V-Fla-O_1** a steady decrease of the emission intensity with increasing temperature was detected with a significanly higher intensity in the Lam_{Col} phase as compared to the less ordered SmA phase. For **O_1-iV-Fla-O_1** a plateau-like emission was reached upon heating shortly before entering the Lam_{Col} phase. In contrast, **O_2-Fla-O_1** displayed a steep decrease of the intensity before reaching a plateau in the Lam_{Col} and SmA phase. That means that the emission in the Lam_{Col} (and in some cases in the SmA) phase remains independent from the

temperature. As suggested by Douce [52] this plateau-like behaviour in the lamellar phase and the strong emission of calamitic flavylium salts might be caused by intercalating ion pairs avoiding π-π stacking and thus fluorescence quenching through the formation of H-aggregates. Douce reported *N*-naphthyl-*N*-benzylimidazolium salts, where the intercalation of the side chains into the aromatic stacks resulted in highly emissive bulk materials [53,54].

Conclusion

Taking inspiration from the supramolecular aggregate based on metal chelates of anthocyanins, which is the origin of the natural pigment cornflower blue, we studied flavylium salts decorated with lipophilic alkoxy or thioether side chains resulting in novel liquid crystalline emissive dyes. The experimental results, which were complemented by X-ray crystallographic data, NMR investigations of the aggregates in solution and quantum chemical calculations revealed that among this class of dyes particularly those members with a calamitic molecular architecture and a lamellar (preferably Lam_{Col} over SmA) liquid crystalline phase indeed show a pronounced emission both in solution and the ordered bulk state.

Author Information

Corresponding Author: sabine.laschat@oc.uni-stuttgart.de

Present Address: Universität Stuttgart, Institut für Organische Chemie, Pfaffenwaldring 55, D-70569 Stuttgart, Germany.

Acknowledgements

Generous financial support by the Deutsche Forschungsgemeinschaft (DFG grants # La 907/17-2, La 907/20-1 SNAPSTER), the Deutsche Akademische Austauschdienst (DAAD PHC Procope, WELCHYNA) Ministerium für Wissenschaft, Forschung und Kunst des Landes Baden-Württemberg, the Bundesministerium für Bildung und Forschung (shared

instrumentation grant # 01 RI 05177), the Studienstiftung des deutschen Volkes (PhD fellowship for J.A. Knöller) and the Carl-Schneider-Stiftung Aalen (shared instrumentation grant) is gratefully acknowledged.

References

[1] Prevot ME, Vanegas JP, Hegmann E. Emissive Nanomaterials and Liquid Crystals, in 21st Century Nanoscience – A Handbook. Boca Raton: CRC Press; 2020.

[2] Wang Y, Shi J, Chen J, et al. Recent progress in luminescent liquid crystal materials: design, properties and application for linearly polarised emission. J Mater Chem C. 2015;3:7993–8005.

[3] V Voskuhl J, Giese M. Mesogens with aggregation- induced emission properties: Materials with a bright future. Aggregate. 2022;3:e124.

[4] Pina F, Melo MJ, Laia CAT, et al. Chemistry and applications of flavylium compounds: a handful of colours. Chem Soc Rev. 2012;41:869–908.

[5] Goto T, Kondo T. Structure and Molecular Stacking of Anthocyanins—Flower Color Variation. Angew Chem Int Ed Engl. 1991;30:17–33.

[6] Roth K. Die Suche nach dem Blau der „Blauen Blume “ Chemie für Romantiker. Chem Unserer Zeit. 2018;52:192–200.

[7] Otegui MS. Imaging Polyphenolic Compounds in Plant Tissues. In: Reed JD, Freitas VAP, Quideau S, editors. Recent Adv Polyphenol Res. 1st ed. Wiley; 2021:281–295.

[8] Quina FH, Moreira PF, Vautier-Giongo C, et al. Photochemistry of anthocyanins and their biological role in plant tissues. Pure Appl Chem. 2009;81:1687–1694.

[9] Li J, Wang B, He Y, et al. A review of the interaction between anthocyanins and proteins. Food Sci Technol Int. 2021;27:470–482.

[10] Lemos M, Sárniková K, Bot F, et al. Use of Time-Resolved Fluorescence to Monitor Bioactive Compounds in Plant Based Foodstuffs. Biosensors. 2015;5:367–397.

[11] Silva GTM, da Silva KM, Silva CP, et al. Highly fluorescent hybrid pigments from anthocyanin-and red wine pyranoanthocyanin-analogs adsorbed on sepiolite clay. Photochem Photobiol Sci. 2019;18:1750–1760.

[12] Merzlyak MN, Melø TB, Naqvi KR. Effect of anthocyanins, carotenoids, and flavonols on chlorophyll fluorescence excitation spectra in apple fruit: signature analysis, assessment, modelling, and relevance to photoprotection. J Exp Bot. 2008;59:349–359.

[13] Bartosz G, Grzesik-Pietrasiewicz M, Sadowska-Bartosz I. Fluorescent products of anthocyanidin and anthocyanin oxidation. J Agric Food Chem. 2020;68:12019–12027.

[14] Ghiman R, Nistor M, Focșan M, et al. Fluorescent polyelectrolyte system to track anthocyanins delivery inside melanoma cells. Nanomaterials. 2021;11:782.

[15] Amogne NY, Ayele DW, Tsigie YA. Recent advances in anthocyanin dyes extracted from plants for dye sensitized solar cell. Mater Renew Sustain Energy. 2020;9:1–16.

[16] Willstätter R, Everest AE. Untersuchungen über die Anthocyane. I. Über den Farbstoff der Kornblume. Justus Liebigs Ann Chem. 1913;401:189–232.

[17] Shibata K, Shibata Y, Kasiwagi I. Studies on anthocyanins: color variation in anthocyanins. J Am Chem Soc. 1919;41:208–220.

[18] Robinson R, Robinson GM. The colloid chemistry of leaf and flower pigments and the precursors of the anthocyanins. J Am Chem Soc. 1939;61:1605–1606.

[19] Bayer E, Egeter H, Fink A, et al. Komplexbildung und blütenfarben. Angew Chem. 1966;78:834–841.

[20] Asen S, Horowitz RM. Apigenin 4′-O-β-d-glucoside 7-O-β-d)-glucuronide: The copigment in the blue pigment of Centaurea cyanus. Phytochemistry. 1974;13:1219–1223.

[21] Kondo T, Ueda M, Tamura H, et al. Composition of protocyanin, a self- assembled supramolecular pigment from the blue cornflower, Centaurea cyanus. Angew Chem Int Ed Engl. 1994;33:978–979.

[22] Shiono M, Matsugaki N, Takeda K. Structure of the blue cornflower pigment. Nature. 2005;436:791–791.

[23] Kondo T, Ueda M, Isobe M, et al. A new molecular mechanism of blue color development with protocyanin, a supramolecular pigment from cornflower, Centaurea cyanus. Tetrahedron Lett. 1998;39:8307–8310.

[24] Takeda K. Blue metal complex pigments involved in blue flower color. Proc Jpn Acad Ser B. 2006;82:142–154.

[25] Kapernaum N, Lange A, Ebert M, et al. Current topics in ionic liquid crystals. ChemPlusChem. 2022;87:e202100397.

[26] Goossens K, Lava K, Bielawski CW, et al. Ionic Liquid Crystals: Versatile Materials. Chem Rev. 2016;116:4643–4807.

[27] Mansueto M, Laschat S. Handbook of Liquid Crystals. In: Goodby JW, Tschierske C, Gleeson HF, et al., editors. Handb Liq Cryst Vol 6. 2nd ed. Weinheim: Wiley-VCH; 2014. p. 231–280.

[28] Axenov KV, Laschat S. Thermotropic Ionic Liquid Crystals. Materials. 2011;4:206–259.

[29] Douce L, Suisse J-M, Guillon D, et al. Imidazolium-based liquid crystals: a modular platform for versatile new materials with finely tuneable properties and behaviour. Liq Cryst. 2011;38:1653–1661.

[30] Chen S, Eichhorn SH. Ionic Discotic Liquid Crystals. Isr J Chem. 2012;52:830–843.

[31] Salikolimi K, Sudhakar AA, Ishida Y. Functional Ionic Liquid Crystals. Langmuir. 2020;36:11702–11731.

[32] Martinetto Y, Pégot B, Roch-Marchal C, et al. Designing Functional Polyoxometalate-Based Ionic Liquid Crystals and Ionic Liquids. Eur J Inorg Chem. 2020;2020:228–247.

[33] Sigaud G, Hardouin F, Gasparoux H, et al. The Smectic a Phases of Some Long Chain Substituted Diaryl-2, 6 Pyrylium and Thiopyrylium Salts. Mol Cryst Liq Cryst. 1983;92:217–224.

[34] Veber M, Jallabert C, Strzelecka H, et al. Heteroaromatic Salts Exhibiting Thermotropic Liquid Crystalline Properties. Mol Cryst Liq Cryst. 1986;137:373–379.

[35] Strzelecka H, Jallabert C, Veber M. Mesomorphism of Heteroaromatic Salts: Influence of the Number of Flexible Chains. Mol Cryst Liq Cryst Inc Nonlinear Opt. 1988;156:355–359.

[36] Strzelecka H, Jallabert C, Veber M, et al. Synthese Efficace de Composes Aromatiques Polyalcoxyles. Mol Cryst Liq Cryst Inc Nonlinear Opt. 1988;156:347–353.

[37] Markovitsi D, Lécuyer I, Clergeot B, et al. Photophysical properties of discogenic triaryl pyrylium salts excimer migration in columnar liquid crystals. Liq Cryst. 1989;6:83–92.

[38] Ecoffet C, Markovitsi D, Jallabert C, et al. Columnar liquid crystals of triaryl pyrylium salts: experimental and theoretical study of photophysical properties. Thin Solid Films. 1994;242:83–87.

[39] Pérez J, Vandevyver M, Strzelecka H, et al. In plane and out of plane anisotropy in Langmuir-Blodgett films of discogenic molecules. Liq Cryst. 1993;14:1627–1634.

[40] Veber M, Berruyer G. Ionic liquid crystals: synthesis and mesomorphic properties of dimeric 2, 4, 6-triarylpyrylium tetrafluoroborates. Liq Cryst. 2000;27:671–676.

[41] Wu D, Pisula W, Haberecht MC, et al. Oxygen-and sulfur-containing positively charged polycyclic aromatic hydrocarbons. Org Lett. 2009;11:5686–5689.

[42] Timmons DJ, Jordan AJ, Kirchon AA, et al. Asymmetric flavone-based liquid crystals: synthesis and properties. Liq Cryst. 2017;44:1436–1449.

[43] Forschner R, Knelles J, Bader K, et al. Flavylium salts: a blooming core for bioinspired ionic liquid crystals. Chem Eur J. 2019;25:12966–12980.

[44] Bora P, Bora B, Bora U. Recent developments in synthesis of catechols by Dakin oxidation. New J Chem. 2021;45:17077–17084.

[45] Knöller JA, Forschner R, Frey W, et al. Chasing Self- Assembly of Thioether- Substituted Flavylium Salts in Solution and Bulk State. ChemPhysChem.2022;23: e202200154.

[46] Jankowiak A, Debska Ż, Romański J, et al. Synthesis of 3, 4-dialkylsulfanyl-and 3, 4, 5-trialkylsulfanyl derivatives of bromobenzene and benzaldehyde. J Sulfur Chem. 2012;33:1–7.

[47] Zheng Q, He GS, Prasad PN. Novel two-photon-absorbing, 1, 10-phenanthroline-containing π-conjugated chromophores and their nickel (II) chelated complexes with quenched emissions. J Mater Chem. 2005;15:579–587.

[48] Cardinaels T, Ramaekers J, Nockemann P, et al. Rigid tetracatenar liquid crystals derived from 1, 10-phenanthroline. Soft Matter. 2008;4:2172–2185.

[49] Cruz C, Heinrich B, Ribeiro AC, et al. Structural study of smectic A phases in homologous series of N-alkylpyridinium alkylsulphates. Liq Cryst. 2000;27:1625–1631.

[50] Bruce DW. Calamitics, cubics, and columnars liquid-crystalline complexes of silver (I). Acc Chem Res. 2000;33:831–840.

[51] Woodford JN. A DFT investigation of anthocyanidins. Chem Phys Lett. 2005;410:182–187.

[52] Douce L, personal communication at ILMAT VI, Obernai, France, 2021.

[53] del Giudice N, l'Her M, Scrafton E, et al. Luminescent Ionic Liquid Crystals Based on Naphthalene- Imidazolium Unit. Eur J Org Chem. 2021;2021:2091–2098.

[54] Berthiot R, del Giudice N, Douce L. Luminescent Imidazolium Salts as Bright Multi- Faceted Tools for Biology. Eur J Org Chem. 2021;2021:4099–4106.